

Finite Element Simulation of Thermal Residual Stress in TLP Bonding of Ni-base Superalloy

Ruaa H K AL-Nafeay

Department of Metallurgical Eng., College of Materials Engineering, University of Babylon, Babil, Iraq.

Ahmed O AL-Roubaiy

Department of Metallurgical Eng., College of Materials Engineering, University of Babylon, Babil, Iraq.

H Omidvar

Department of Materials and Metallurgical Engineering, Amirkabir University of Technology, Tehran, Iran.

Abstract:

In this article, A three-dimensional finite element model was used to study localized thermal residual stresses generated in the Transient liquid phase (TLP) bonding of Ni-base superalloy (IN738LC, IN939) which are the main materials of gas turbine blades, with BNi-2 foil as a filler alloy. The models simulated the thermal residual stresses that developed as a joint is cooled in the furnace from the bonding temperature (1120 °C) to room temperature (25 °C) during 4 hr. (1440 sec), using Abaqus-CAE software. The same materials and geometries that were tested experimentally were used in the model. The results show larger thermal residual stress is generated in the interface (bonding zone) and the stress decreases gradually to both ends due to property mismatch between the base metal and filler alloy, These stress are below the yield point of base metals in all the types of bonding in this study.

Keywords: Finite element model, Nickel (Ni) based superalloys, Gas turbine blade, Transient liquid phase(TLP).

INTRODUCTION

Because of its great strength and corrosion resistance, nickel-based superalloys are utilized at high operating temperatures of the turbine. To obtain increased efficiency and production, current gas turbine engines need to utilize higher gas pressures and operating temperatures [1,2]. superalloys based on nickel (IN738, IN939) are obtained by precipitation hardening from gamma prime phase ($\text{Ni}_3(\text{Al}, \text{Ti})$), and carbides (MC type) are widely described as materials meeting these requirements, and they have found a considerable application in gas turbine blades and vanes [3]. Andersson. [4] showed that The presence of precipitates (such as metallic carbides and intermetallic particles) improves the operation at high temperatures but affects the weldability of these alloys. Precipitation hardened of superalloys based on nickel (with high Al and Ti concentrations) is very hard to weld [5-7]. Gonzalez et al. [8] shown the influence of microcrack development in the HAZ by Residual stresses and material cleanness. As a result, residual stresses are important in both mechanical performance, and micro-cracking of the weld and heat-affected zone of IN939, and IN738LC during heat treatments. When no external pressures are applied, Residual stresses are self-balancing stresses inside a structure. Material processing and manufacturing procedures can result in a residual stress field (RSF) in the finished component. Traditional welding procedures for metallic structures generate one of the most undesired RSF, where high tensile residual-stresses RS occur from a persistent mismatch between the near-weld zone and the body of the workpiece [9]. Premature failure of a component is typically caused by post-weld tensile residual stresses, which show themselves as faster crack propagation at the weld zone [9,10].

The use of transient liquid phase bonding (TLPB) to link high-temperature materials with excellent integrity is a good option. Nonetheless, several difficulties are discovered during TLP bonding as a result of thermal mismatch and temperature distribution. Transient Liquid Phase Bonding (TLPB) is a joining technique used to combine similar and dissimilar metals that cannot be joined using traditional fusion welding methods. The bonding procedure results in a joint that is resistant to surface oxides and geometrical defects. This bonding technique has a wide range of applications in the aerospace industry, including turbine engine maintenance and manufacture, as well as fuel cladding in nuclear power stations. [11-13].

The filler alloy (interlayer) is placed between the base metals and maybe thin foil, paste, or powder. The melting point should be less than the melting point of the base metal substance. The overall specimen is placed in a furnace and heated below the melting

point of the base metals for a fixed length of time for isothermal solidification at the bonding temperature. The remelting temperature is above the original melting temperature of the base metals. [11-15]. In the topic of superalloy based on nickel bonding, much of the research focused on the experimental investigation which focused largely on phase transitions, changes in the microstructures following bonding, preheating effects, and heat treatment after bonding [16–19]. However, only a few research have been conducted on modeling and numerical analysis of the Ni-based bonding process.

Hynes and Raja [20] studied numerical simulation of ceramic/metal TLP bonding process, According to simulation tests, lowering the bonding temperature increases beneficial temperature distribution and, as a result, the joint efficiency of graphite/copper joints. Danis et al. [21] investigated the relationship between mechanical, thermal, and metallurgical parameters in the region of HAZ. by examining the influence of different IN738 welding conditions. They observed that reducing welding RS was the most significant element in preventing cracking in the heat-affected zone area, highlighting the importance of welding RS prediction using an accurate and comprehensive finite element model. Bonakdar et al. [22] studied the electron beam welding of an IN 713LC gas turbine blade using finite element modeling. In this present paper, thermal residual stress (TRS) of IN939, and IN738 joints using BNi-2 as a filler metal were Simulated. The Simulation of TLP bonding for Ni-base superalloy and prediction of TRS through the cooling joint from bonding temperature to room temperature is the major purpose of this work, which is relatively new, and similar works in this field are quite limited in the literature.

MODEL CHARACTERISTICS

A three-dimensional finite element model was built. The Model containing the geometry of the three-dimension solid component partitions with different material properties (base metals and filler alloy), their assembly, and the mesh characteristics in addition to boundary conditions. The dimensions of the base metal parts in the joint sample are (0.01m×0.01m×0.005m) for each base metal parts and BNi-2 foil having dimensions (0.01m×0.01m×0.00007m) is used as interlayer for the similar and dissimilar joint that used in this simulation. The geometry and dimensions used for each part in the model were identical to the dimensions used for the samples in the experimental work as shown in “figure 1”. “Figure 2” shows the modeled geometry.

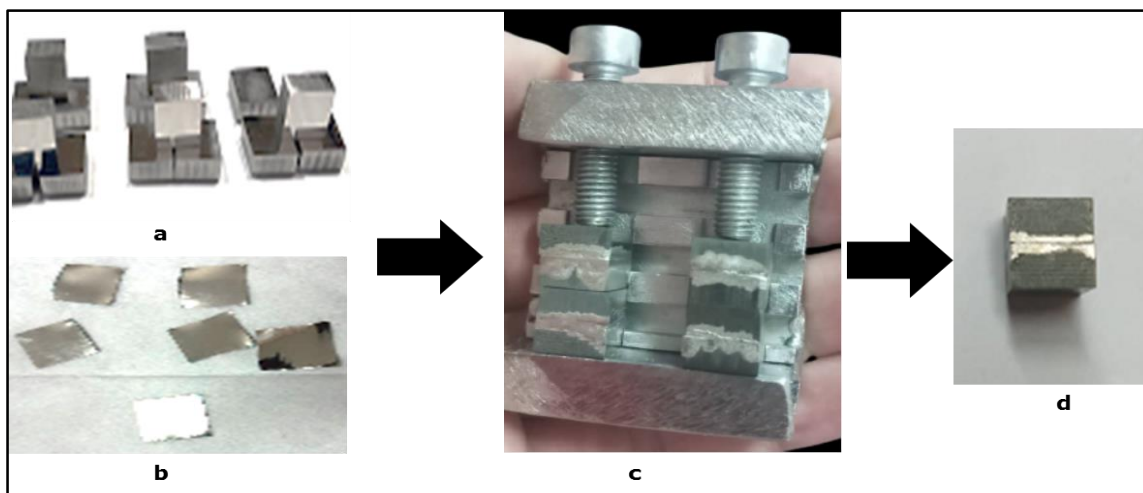


FIGURE 1: The experimental work for the TLP bonding: a: base metal in diminutions (0.01m×0.01m×0.005m), b: filler metal in diminutions (0.01m×0.01m×0.00007m), c: assembly after bonding in the vacuum furnace (10⁻⁵Toor), d: a bone sample with dimensions (0.01m×0.01m×0.01m).

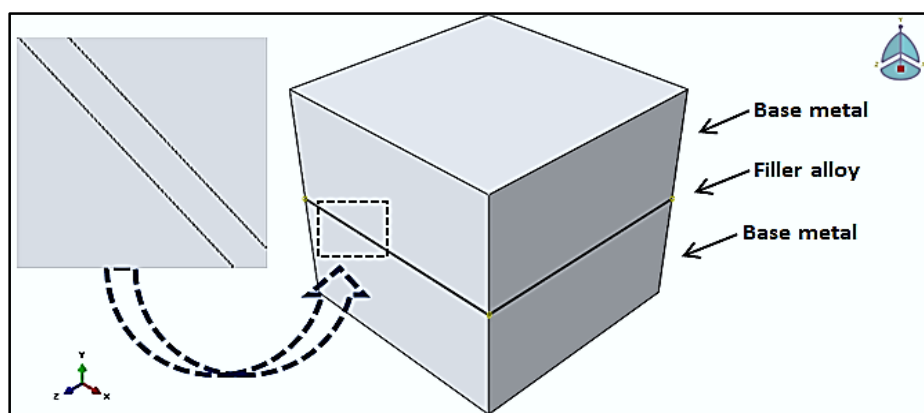


FIGURE 2: Geometry definition of the different material partition zones used for the model of the joint.

ASSUMPTIONS

1. Only thermal loading is applied.
2. The ambient temperature was considered to be between 20 and 25 degrees Celsius.
3. The materials are stress-free at the joining temperature.
4. The filler alloy was assumed to exactly fill the gap between the base metals at high temperature without diffusion between the filler alloy and base metal because of the difficulty in representing the diffusion in the model.
5. Uniform cooling and the base metals and filler alloy in dissimilar and similar materials are perfectly bonded at the interface and free from any defects.
6. Temperature equilibration throughout the system occurs instantaneously.
7. The models simulated the thermal residual stresses that develop as a joint is cooled from bonding temperature to 25 °C.

MATERIAL PROPERTIES

The materials are base metals (IN738LC, and IN939), and BNi-2 as the filler metal. The temperature-dependent properties (thermal and mechanical) for IN738LC, IN939, and Bni-2 (Bonding zone) were extracted from the references [23-27]. Which are listed in “Tables 1, 2, and 3”.

TABLE 1: Thermo-mechanical properties for IN738LC used as a base metal in the modeling of IN738LC/BNi-2/IN738LC, and IN738LC/BNi-2/IN939 [23,24].

Temperature (C°)	Yield stress (MPa)	Young modulus (GPa)	Poisson ratio	Coefficient of thermal expansion, (1/C°)
24	950	200.63	0.28	6.45×10^{-6}
93	941	195.12	0.27	6.45×10^{-6}
204	900	190.29	0.27	6.75×10^{-6}
426	876	179.26	0.28	7.55×10^{-6}
649	822	167.54	0.30	8.05×10^{-6}
760	793	157	0.30	8.25×10^{-6}
871	582	151	0.29	8.55×10^{-6}
982	345	141	0.30	8.85×10^{-6}
1093	291	150	0.29	9.15×10^{-6}
1204	105	120	0.30	9.45×10^{-6}

TABLE 2: Thermo-mechanical properties for IN939 used as a base metal in the modeling of IN939/BNi-2/IN939, and IN738LC/BNi-2/IN939 [25,26].

Temperature (C°)	Yield stress (MPa)	Young modulus (GPa)	Poisson ratio	Coefficient of thermal expansion, (1/C°)
20	700	217	0.27	11×10^{-6}
100	667	212	0.27	11.3×10^{-6}
200	644	206	0.28	12.2×10^{-6}
400	615	195	0.29	13.3×10^{-6}
600	546	183	0.29	14.2×10^{-6}
800	512	170	0.3	14.6×10^{-6}
1000	366	151	0.31	16.4×10^{-6}
1200	45	143	0.31	19.7×10^{-6}

TABLE 3: Thermo-mechanical properties for BNi-2 used as filler metal in the modeling [27].

Temperature (C°)	Yield stress (MPa)	Young modulus (GPa)	Poisson ratio	Coefficient of thermal expansion, (1/C°)
20	424	205.1	0.29	13.5×10^{-6}
400	368	183.2	0.30	16.8×10^{-6}
800	255	161	0.32	19.9×10^{-6}
900	160	127.6	0.32	21.3×10^{-6}

BOUNDARY CONDITIONS IN THE MODEL

To simulate the thermal residual stress of the bonded samples, the model was assumed to be subjected to thermal load. The thermal load applied to the 3D model is temperature changes from the bonding temperature (1120 °C) to room temperature (25 °C) during 4 hr (1440 sec) as shown in “figure 3”. To avoid mismatching during the TLP bonding in a vacuum furnace, the base

metals and filler metal should be assembled and fixed tightly. The bottom face was constrained in Y-direction. As a result, This prevented rigid movement. The top of the face for the model in Y-direction was fixed to simulate the clamping.

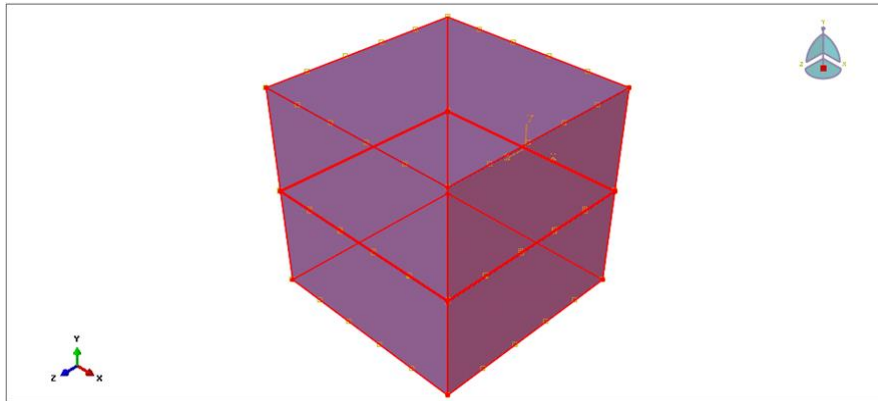


FIGURE 3: Thermal load of the model

MESH BUILDING

A hexahedral structured mesh element was created in all the regions of the samples. A good finite element mesh may be defined as the mesh with a minimum number of elements necessary to provide acceptable solution accuracy. Therefore, the size of meshes are used in this model:

1. Base metals meshed in approximate element size 0.0005m for the base metal parts in the 3D model as shown in "figure 4a".
2. Filler alloy meshed in size of element 0.00001m for the interlayer in the 3D model as shown in "figure 4b".

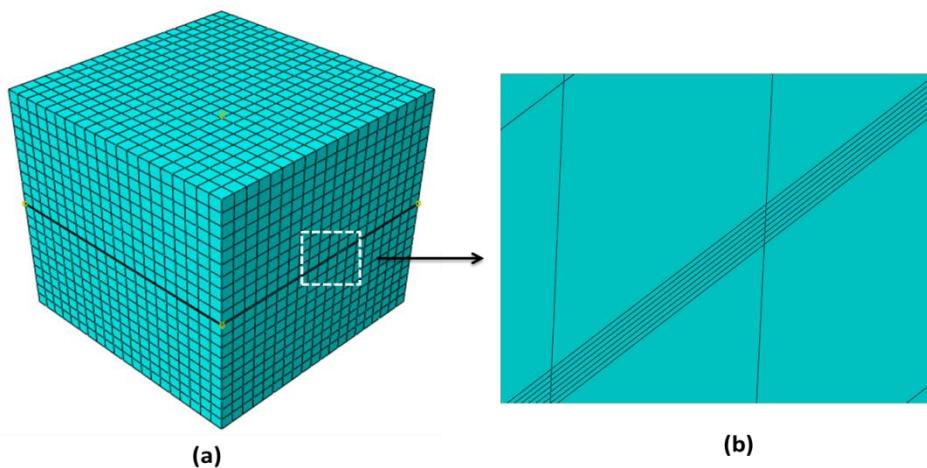


FIGURE 4: a: Meshing size of the mode, b: Mish size of the interlayer

RESULTS AND DISCUSSION

The finite element models provided a qualitative understanding of the thermal residual stress state in the TLP bonding with 0.00007m interlayer thickness undercooling in the furnace from bonding temperature 1120°C to room temperature 25°C. The simulation of thermal residual stress is important in the bonding between the base metal and the interlayer (filler alloy) to predict the lifetime of the joint to take consideration that in fabrication them or repairing these materials.

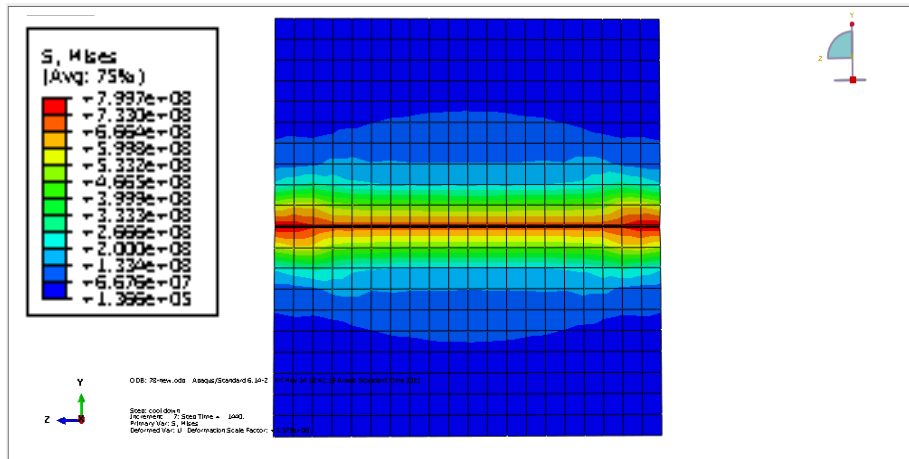
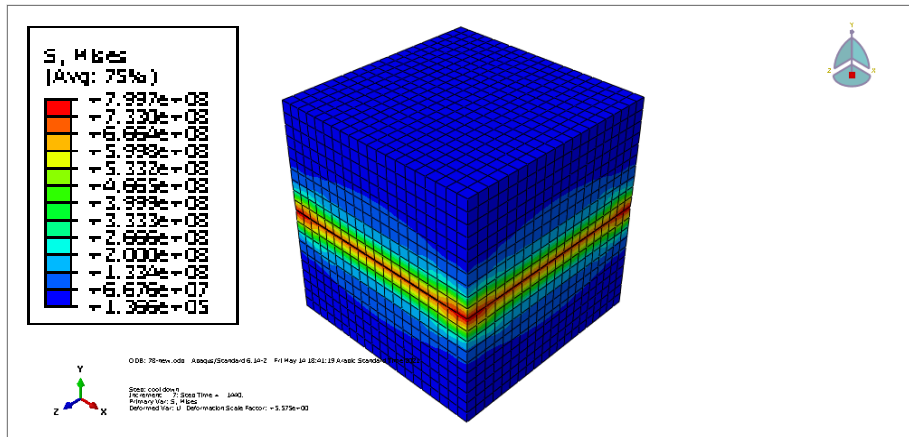


FIGURE 5: Von-Mises residual stress in TLP bonding for similar IN738LC.

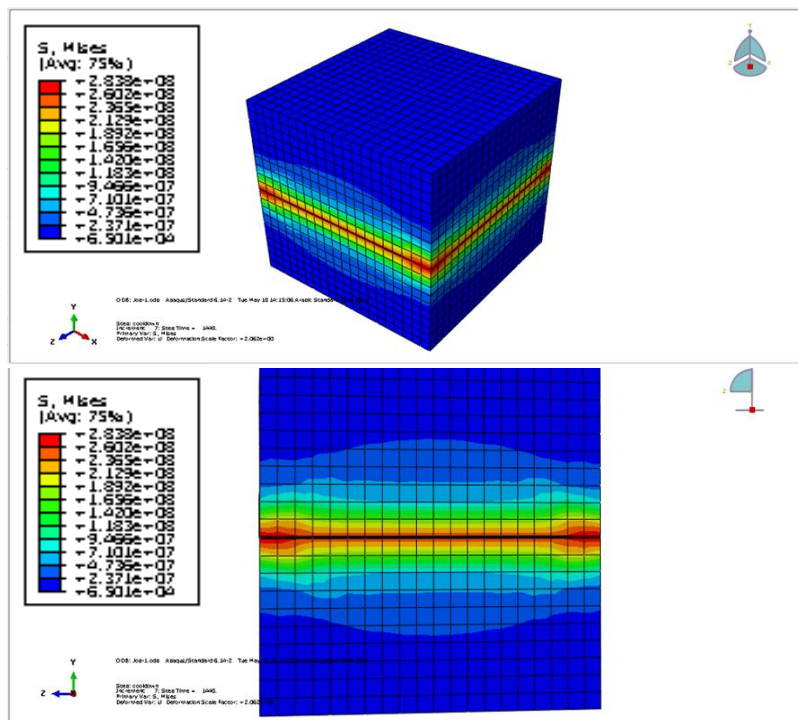


FIGURE 6: Von-Mises residual stress in TLP bonding for similar IN939.

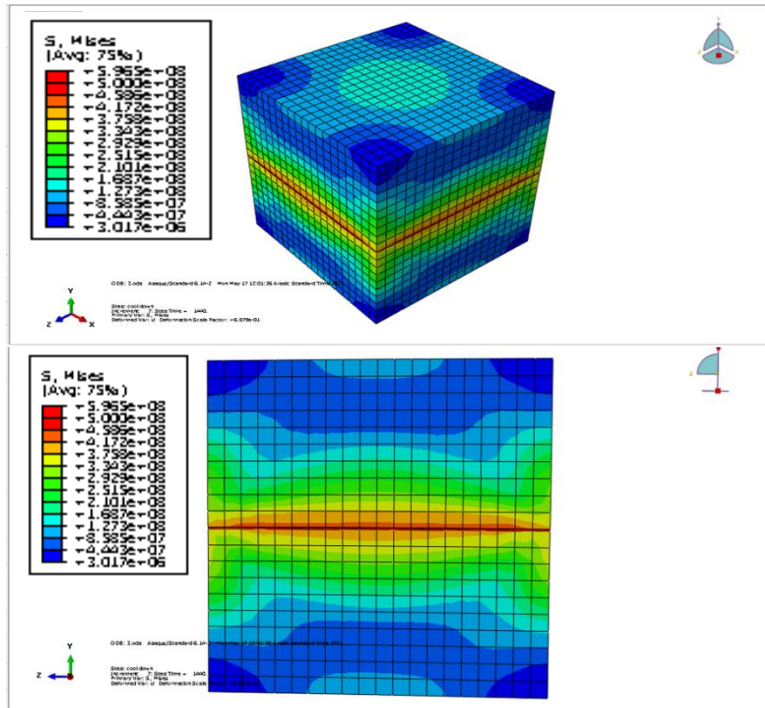


FIGURE 7: Von-Mises residual stress in TLP bonding for dissimilar IN738LC/IN939.

The results show that the von-mises equivalent stress for the TLP bonding of Ni-base superalloy (similar IN738LC, similar IN939, and dissimilar IN738LC/IN939) mostly concentrated at the interface (bonding zone) between the filler alloy and base metal. This is due to the different properties especially the thermal expansion coefficient between them. It clear that the stress decreases gradually to both ends, this is due to the decreasing the sharpness in material properties change as can be observed in figures (5, 6, 7). These figures show the results for TLP bonding of Ni-base superalloy, it clear that the von-mises stress in IN738LC higher value than the stress of IN939, and in dissimilar (IN738LC/IN939) bonding, the values of stress are high in the side of IN738LC and lower values in the side of IN939. This is due to the difference in thermal expansion coefficient between IN738LC and filler alloy higher than the difference between IN939 and the filler alloy. And as observed in "figure 6" the stress distribution occurred in a larger area dissimilar than the similar bonding.

The figures (8,9,10) show the effect of transition between the filler alloy and base metal. the maximum stress concentrated at the points near the interface and in the center of the interface as can be seen in figures (8,9), and the bond sample in figure 7 for similar IN738 LC shows much higher peak stress than the peaks seen in IN939 bonding in figure 8. While in figure 10 for dissimilar bonding, high-stress concentration near the interface in the side of IN738 LC (upper part) and decrease near the side of IN939 (lower part).

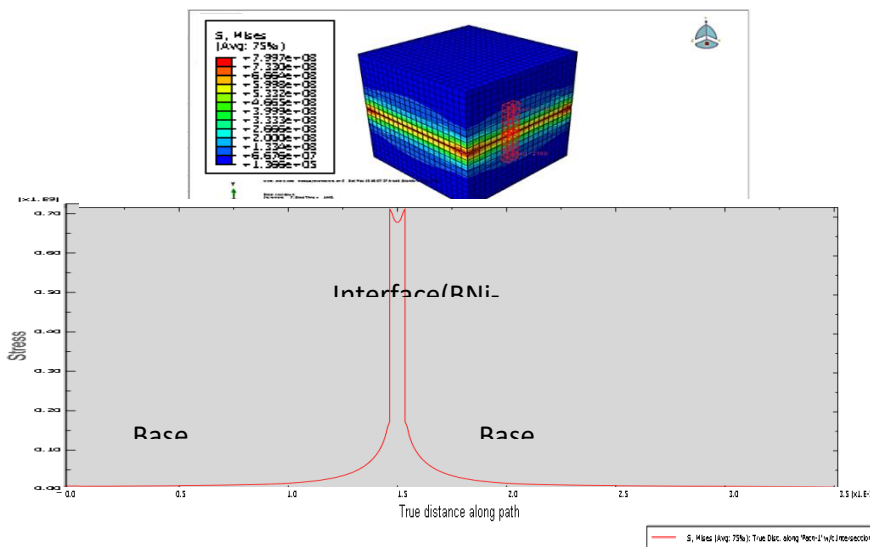


FIGURE 8: Distribution of thermal residual stress perpendicular to the interface for TLP bonding of IN738LC.

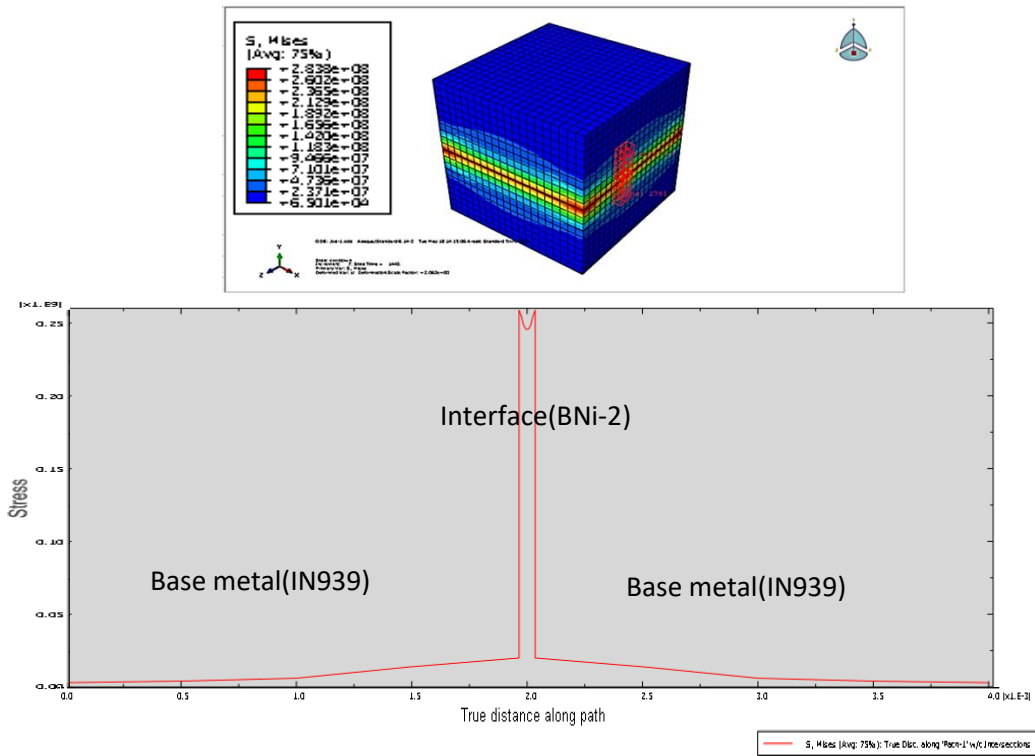


FIGURE 9: Distribution of thermal residual stress perpendicular to the interface for TLP bonding of IN939.

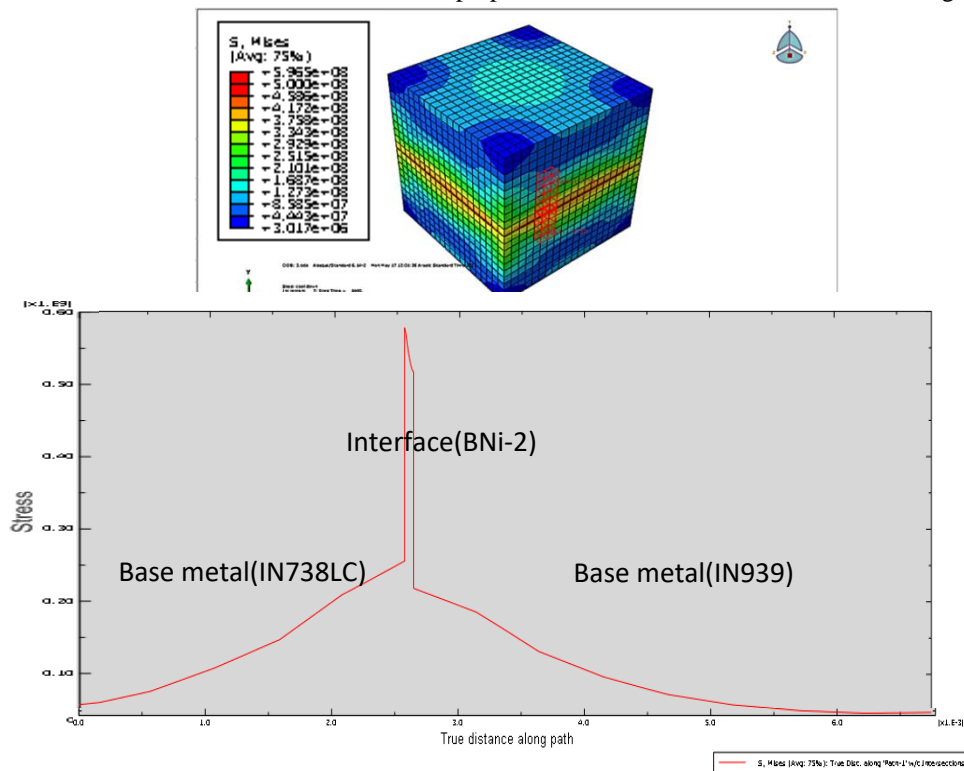


FIGURE 10: Distribution of thermal residual stress perpendicular to the interface for TLP bonding of IN738LC/IN939.

The model results to evaluate the thermal residual stress agrees with the literature results of modeling researches [25, 28 -30]. In all these types of TLP bonding for the similar (IN738LC, IN939) and dissimilar (IN738LC/IN939), the von-mises stress was below the yield point of the base metals. So, these joints are safe, and as mentioned above in assumptions, the filler alloy was

assumed to fill the gap between the base metals at high temperature without diffusion because of the difficulty in representing the diffusion in the model. So, this thermal residual stress is higher than the real stress in experimental due to the effect of inter-diffusion between the base metal and filler alloy makes the gradational in the properties lower, so the stresses in real condition will be much lower than that in the model simulation.

CONCLUSIONS

In the present work, prediction of the thermal residual stress of TLP bonding of Ni-base superalloy during cooled them from bonding temperature to room temperature. Three types of TLP bonding are studied, similar IN738LC, and dissimilar IN738LC/IN939, also similar IN939, were carried out by ABAQUS finite element code. The following conclusion can be made:

1. Large stresses are generated in the interface (bonding zone) due to property mismatch especially thermal expansion coefficient between the base metal and filler metal.
2. In the model of TLP bonding samples, stress distribution showed approximately the same overall behavior with the highest concentration occurring at the region near the interface.
3. For comparison between the stress that generated in similar IN738LC, IN939 and dissimilar IN738LC/IN939, for similar IN738 LC shows much higher peak stress than the peaks in similar IN939 bonding, and for dissimilar, the values of stress are high in the side of IN738LC and lower values in the side of IN939. This is due to the difference in thermal expansion coefficient between IN738LC and filler alloy higher than the difference between IN939 and the filler alloy.
4. The von-mises stresses for all these types of TLP bonding of Ni-base superalloy were below the yield point of the base metals. So, these joints are safe.

REFERENCES

- [1] Kataria, R., Singh, R. P., Sharma, P., & Phanden, R. K. (2020). Welding of superalloys: A review. *Materials Today: Proceedings*.
- [2] Sashank, S. S., Rajakumar, S., Karthikeyan, R., & Nagaraju, D. S. (2020). Weldability, Mechanical Properties and Microstructure of Nickel-Based Super Alloys: a review. In *E3S Web of Conferences* (Vol. 184, p. 01040). EDP Sciences.
- [3] Frank Mevissen and Michele Meo (2019) "A Review of NDT/Structural Health Monitoring Techniques for Hot Gas Components in Gas Turbines" *Sensors*, 19(3), 711.
- [4] Andersson J (2018) Review of weldability of precipitation hardening Ni- and Fe-Ni-based superalloys. In: *Proceedings of the 2018 Superalloy 718 & Derivatives: Energy, Aerospace, and Industrial Applications*. The Minerals, Metals & Materials Society, Pittsburgh, USA, p submitted manuscript.
- [5] Xiong, J., Yuan, L., Zhu, Y., Zhang, H., & Li, J. (2019). Diffusion bonding of nickel-based superalloy GH4099 with pure nickel interlayer. *Journal of Materials Science*, 54(8), 6552- 6564.
- [6] O.Olatunji,(2016), "Transient liquid phase bonding of dissimilar single crystal superalloys by oluwadamilola Akande Olatunji a thesis submitted to the faculty of graduate studies of the The University of Manitoba," University of Manitoba.
- [7] Amiri, D., Sajjadi, S. A., & Kamyabi-Gol, A. (2020). Pre-and post-TLP bond solution treatments: Effects on the microstructure and mechanical properties of GTD-111 superalloy. *Journal of Manufacturing Processes*, 57, 36-47.
- [8] M. A. GonzaLez, D. I. MartiNez, A. PeRez, H. Guajardo and A. Garza, "Microstructural response to heat affected zone cracking of prewelding heat-treated Inconel 939," *Mater. Charact.*, vol. 62, no. 12, pp. 1116–1123, 2011. DOI: 10.1016/j.matchar.2011.09.006.
- [9] Ding, Z., Sun, G., Guo, M., Jiang, X., Li, B., & Liang, S. Y. (2020). Effect of phase transition on micro-grinding-induced residual stress. *Journal of Materials Processing Technology*, 281, 116647.
- [10] Xiao, Z., Chen, C., Zhu, H., Hu, Z., Nagarajan, B., Guo, L., & Zeng, X. (2020). Study of residual stress in selective laser melting of Ti6Al4V. *Materials & Design*, 193, 108846.
- [11] Tarai, U. K., Robi, P. S., & Pal, S. (2018, April). Development of a Novel Ni-Fe-Cr-B-Si Interlayer Material for Transient Liquid Phase Bonding of Inconel 718. In *IOP Conference Series: Materials Science and Engineering* (Vol. 346, No. 1, p. 012048). IOP Publishing.
- [12] Duvall, D. S., Owczarski, W. A., & Paulonis, D. F. (1974), "TLP bonding: a new method for joining heat resistant alloys", *Weld. J.(NY)*, 53(4), 203-214.
- [13] Saleh, A. A. (2019). "Investigating The Microstructure and Mechanical Properties of Brazed Joint of Inconel 738 LC Alloys Bonded by 5Ni 5Ti 90Al Filler Alloy". *IVK-Structural Integrity and Life*, 19(1), 13-17.
- [14] Li, L., & Liu, D. (2021). Complete dissolution of gamma prime via severe plastic deformation in a precipitation-hardened nickel-base superalloy. *Materials Letters*, 284, 128607.
- [15] Aliya, D., Walker, L. W., Montz, E., Pastor, S., Abad, A., Hashim, F. A., ... & Ula, N. (2014). Characterization of the Effects of Active Filler-Metal Alloys in Joining Ceramic-to-Ceramic and Ceramic-to-Metal Materials. In *Defect and Diffusion Forum* (Vol. 354, pp. 167-173). Trans Tech Publications Ltd.
- [16] Doroudi, A., Shamsipur, A., Omidvar, H., & Vatanara, M. (2019). "Effect of transient liquid phase bonding time on the microstructure, isothermal solidification completion and the mechanical properties during bonding of Inconel 625 superalloy using Cr-Si-B-Ni filler metal". *Journal of Manufacturing Processes*, 38, 235-243.

- [17] Ye, Y., Zou, G., Long, W., Jia, Q., Bai, H., Wu, A., & Liu, L. (2019). Diffusion brazing repair of IN738 superalloy with a crack-like defect: microstructure and tensile properties at high temperatures. *Science and Technology of Welding and Joining*, 24(1), 52-62.
- [18] Binesh, B. (2020). Diffusion brazing of IN718/AISI 316L dissimilar joint: Microstructure evolution and mechanical properties. *Journal of Manufacturing Processes*, 57, 196-208.
- [19] Jalilvand, V., Omidvar, H., Shakeri, H. R., & Rahimpour, M. R. (2013). "A study on the effect of process parameters on the properties of joint in TLP-bonded Inconel 738LC superalloy". *Metallurgical and Materials Transactions B*, 44(5), 1222-1231.
- [20] Dr.N.Rajesh Jesudoss Hynes, and M.Karthick Raja (2015). "Numerical Simulation on Influence of Bonding Temperature in Transient Liquid Phase Bonding", *AIP Conf. Proc.* 1728, 020543-1–020543-4; DOI: 10.1063/1.4946594
- [21] Y. Danis, C. Arvieu, E. Lacoste, T. Larrouy and J. M. Quenisset, "An investigation on thermal, metallurgical and mechanical states in weld cracking of Inconel 738LC superalloy," *Mater. Des.*, vol. 31, no. 1, pp. 402–416, 2010. DOI: 10.1016/j.matdes.2009.05.041.
- [22] H. Alipooramirabad, A. Paradowska, R. Ghomashchi and M. Reid, "Investigating the effects of welding process on residual stresses, microstructure and mechanical properties in HSLA steel welds," *J. Manuf. Process.*, vol. 28, pp. 70–81, 2017. DOI:10.1016/j.jmapro.2017.04.030.
- [23] Lee, J. M., Seok, C. S., Lee, D., Kim, Y., Yun, J., & Koo, J. M. (2014). Prediction of thermo-mechanical fatigue life of IN738 LC using the finite element analysis. *International journal of precision engineering and manufacturing*, 15(8), 1733-1737.
- [24] Ogunbiyi, O. F., Salifu, S. A., Jamiru, T., Sadiku, E. R., & Adesina, O. T. (2019, October). Thermo-mechanical simulation of steam turbine blade with spark plasma sintering fabricated Inconel 738LC superalloy properties. In *IOP Conference Series: Materials Science and Engineering* (Vol. 655, No. 1, p. 012046). IOP Publishing.
- [25] Moattari, M., Shokrieh, M. M., Moshayedi, H., & Kazempour-Liasi, H. (2020). Evaluations of residual stresses in repair welding of Ni-based IN939 superalloy. *Journal of Thermal Stresses*, 43(7), 801-815.
- [26] J. B. Wahl and K. Harris, "Advanced Ni-base superalloys for small gas turbines," *Can. Metall. Quart.*, vol. 50, no. 3, pp. 207–214, 2011. DOI: 10.1179/1879139511Y.0000000010.
- [27] Sharma, D. K., Bandyopadhyay, M., Joshi, J., & Chakraborty, A. K. (2020). Determination of Residual Stresses in Ceramic-Metal Brazed Joint using Finite Element Analysis (FEA) and Experimental Validation of the Results. *SAMRIDDHI: A Journal of Physical Sciences, Engineering and Technology*, 12(01), 1-7.
- [28] Moattari, M., Shokrieh, M. M., & Moshayedi, H. (2020). Effects of residual stresses induced by repair welding on the fracture toughness of Ni-based IN939 alloy. *Theoretical and Applied Fracture Mechanics*, 108, 102614.
- [29] Ikpe, A., Oghenefejiro, E. O., & ARIAVIE, G. (2018). Thermo-structural analysis of first stage gas turbine rotor blade materials for optimum service performance. *International journal of engineering and applied sciences*, 10(2), 118-130.
- [30] Jiang, W., Wei, Z., Luo, Y., Zhang, W., & Woo, W. (2016). Comparison of Brazed Residual Stress and Thermal Deformation between X-Type and Pyramidal Lattice Truss Sandwich Structure: Neutron Diffraction Measurement and Simulation Study. *High Temperature Materials and Processes*, 35(6), 567-574.